



HAL
open science

Measurements of Bubble Characteristics: Comparison Between Double Optical Probe and Imaging

Sammy Lewis Kiambi, Anne-Marie Billet, Jean-Baptiste Dupont, Catherine
Colin, Frédéric Risso, Henri Delmas

► **To cite this version:**

Sammy Lewis Kiambi, Anne-Marie Billet, Jean-Baptiste Dupont, Catherine Colin, Frédéric Risso, et al. Measurements of Bubble Characteristics: Comparison Between Double Optical Probe and Imaging. Canadian Journal of Chemical Engineering, 2003, 81 (3-4), pp.764-770. 10.1002/cjce.5450810357 . hal-02057094

HAL Id: hal-02057094

<https://hal.science/hal-02057094v1>

Submitted on 5 Mar 2019

HAL is a multi-disciplinary open access archive for the deposit and dissemination of scientific research documents, whether they are published or not. The documents may come from teaching and research institutions in France or abroad, or from public or private research centers.

L'archive ouverte pluridisciplinaire **HAL**, est destinée au dépôt et à la diffusion de documents scientifiques de niveau recherche, publiés ou non, émanant des établissements d'enseignement et de recherche français ou étrangers, des laboratoires publics ou privés.







Open Archive Toulouse Archive Ouverte

OATAO is an open access repository that collects the work of Toulouse researchers and makes it freely available over the web where possible

This is an author's version published in: <http://oatao.univ-toulouse.fr/21811>

Official URL : <https://doi.org/10.1002/cjce.5450810357>

To cite this version:

Kiambi, Sammy Lewis  and Billet, Anne-Marie  and Dupont, Jean-Baptiste and Colin, Catherine and Risso, Frédéric  and Delmas, Henri  *Measurements of Bubble Characteristics: Comparison Between Double Optical Probe and Imaging*. (2003) The Canadian Journal of Chemical Engineering, 81 (3-4). 764-770. ISSN 0008-4034

Any correspondence concerning this service should be sent to the repository administrator: tech-oatao@listes-diff.inp-toulouse.fr

Measurements of Bubble Characteristics: Comparison Between Double Optical Probe and Imaging

S.L. Kiambi¹, Anne-Marie. Duquenne¹, J-B. Dupont², C. Colin², F. Risso² and Henri Delmas^{1*}

¹ *Laboratoire de Génie Chimique de Toulouse, Parc d'Activités de Basso Cambo, 5 rue Paulin Talabot, 31106 Toulouse, France*

² *Institut de Mécanique des Fluides de Toulouse, 1 Allée du Professeur Camille Soula, 31400 Toulouse, France*

An accurate local measurement of two-phase flow characteristics is important for the development of two-phase flow models. Computational fluid dynamics (CFD) is developing rapidly in chemical engineering and models arising for these simulations need accurate experimental data to be validated. In gas-liquid contactors, precise knowledge of interfacial area is essential for quantification of mass transfer efficiency. Multi-sensor needle probes are a very common tool for gas-liquid local dynamics investigations in high void fraction bubbly flows where most other techniques have failed. The current study concerns a double optical probe but some recent work has involved miniaturized four-sensor conductivity probes (Kim et al., 2001) which provide similar signals. However, the results concerning the probe intrusiveness are relevant to most existing probes.

From these probes, local two-phase flow parameters such as bubble frequency, bubble velocity, void fraction, bubble chord lengths, bubble size and interfacial area concentration can be deduced. Interfacial area can be evaluated through statistical correlations incorporating bubble frequency, bubble velocity distribution and a correction factor based on the impact (hitting) angle described by the normal interfacial velocity vector and probe vertical axis (Revankar and Ishii, 1992; Dias et al., 2000). However, Kiambi et al. (2001) showed in a recent study that the interfacial area, when evaluated by this way in a highly dispersed flow, is underestimated with respect to the classical $6\alpha_g/d_{Sauter}$ formula. The inaccuracies are attributed to bubble velocity overestimation due to bubble spherical shape assumption, bubble surface deformation, and missed bubbles (bubbles that miss at least one of the sensors). Furthermore, it is not clear from previous studies whether the velocity to be taken into account to characterise interfacial area transport, has to be the bubble interface velocity, the vertical velocity or that of its centre of mass.

The objectives of the authors are to put in evidence bubble-probe interaction and the related disturbance, and to evaluate the corresponding discrepancies in the measured parameters.

The path of the bubble as it ascends in water is filmed by two high-speed cameras and the resulting signal is recorded by means of a double optical probe electronic module.

The objective of this study is to evaluate the accuracy of double optical probe technique in local two-phase flow measurements. Able to provide both bubble velocity, chord length, and gas hold-up, this technique involves nevertheless delicate signal treatment procedures and, being intrusive, depends on probe tips configurations and sizes. During probe-bubble interactions, bubble surface is occasionally deformed and this can complicate measurements analysis. The current study is focussed on the rise of single bubbles of known sizes in still water (equivalent diameter of 2.15mm and 4.5mm). Bubble parameters obtained from digital image processing method and from a double optical probe are compared statistically.

L'objectif de ce travail est de quantifier la précision de la sonde optique à deux fibres pour des mesures locales en écoulements biphasiques. Bien que pouvant fournir la vitesse de bulle, sa longueur de corde, et le taux de gaz, cette technique nécessite des procédures de traitement du signal délicates, et étant intrusive, elle dépend des forme et taille de la sonde. On visualise comment l'interaction sonde-bulle perturbe la forme et la vitesse de la bulle. Pour deux diamètres équivalents, 2,15 et 4,5mm, les paramètres de bulles uniques en ascension dans de l'eau au repos, obtenus par sonde optique double et par traitement d'images, sont comparés statistiquement.

Keywords: Double optical probe, gas hold-up, bubble velocity, image processing.

Experimental Set-up and Measurement Procedure

Experimental Set-up

The set-up consists of a test section in an open tank of 700mm height with a square cross-section of 150mm as shown in Figure 1. To allow full optical access the four sides of the tank are made of glass. For air injection two stainless steel capillary tubes are located at the mid-point of the tank base. These capillaries of 0.33mm and 1mm internal diameters produce bubbles of 2.15mm and 4.5mm equivalent diameters respectively. Air is injected at low flow rates to ensure

*Author to whom correspondence may be addressed. E-mail address: henri.delmas@ensigt.fr

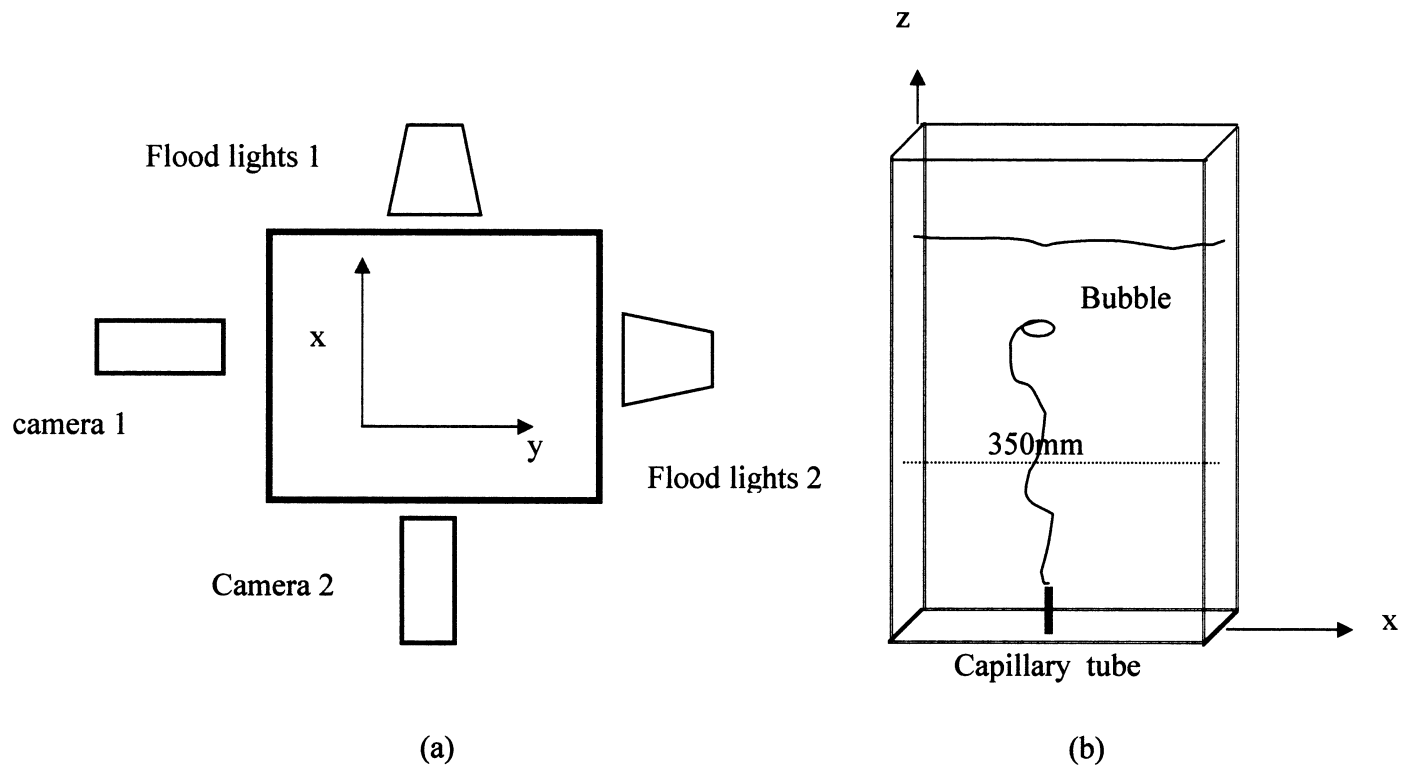


Figure 1. Experimental set-up.

that the bubble volume at detachment is controlled by static balance between surface tension and buoyancy forces. Bubbling frequency is kept low enough to avoid the wake effects of preceding bubbles.

Double Optical Fibre Probe

A double optical probe (RBI) is mounted into the tank at a height of 350mm above injection level where the bubbles have

already attained their terminal velocity. The probe tips have a diameter of 40 μ m and are 3.1mm from each other (Figure 2a). The image acquisition is synchronised with the optical probe acquisition such that the signal from the first probe sensor triggers the image acquisition. This means that only bubbles pierced by the first fibre are filmed.

The measurement principle of the probe technique lays on the difference of refraction indexes between the two media (air and water). The sampling frequency of the probe is 6.25kHz which ensures accurate signal registration. Each of the two optical sensors is connected to its own measuring circuit and therefore each sensor is used as an independent phase identifier. A sample of two signals recorded is shown in Figure 2b. Phase discrimination is done by setting a threshold on the output signal as shown on the figure.

From the output signal of the probe, the local gas hold-up and the local bubbling frequency can be evaluated (Liu and Bankoff, 1993) Local gas hold-up at a point P in the gas/liquid flow is given by $\alpha_p = \sum_1^{nb} t_R / T$ where nb is the total number of bubbles pierced by fibre1, T is the total measuring time and t_R is the bubble residence time on the first probe ($t_R = t_{12} - t_{11}$, see Figure 2b). A statistical analysis based on cross correlation of both signals (Kamp, 1996) identifies bubbles pierced by both probe tips and for these bubbles, the interfacial velocity is obtained from the bubble transit time between the two probe tips $t_{21} - t_{11}$: interfacial bubble velocity from the probe is evaluated from $V_{pi} = l_{12} / (t_{21} - t_{11})$ where l_{12} is the distance between the two probe tips. Bubble chords lengths are equal to: $(t_{12} - t_{11}) V_{pi}$.

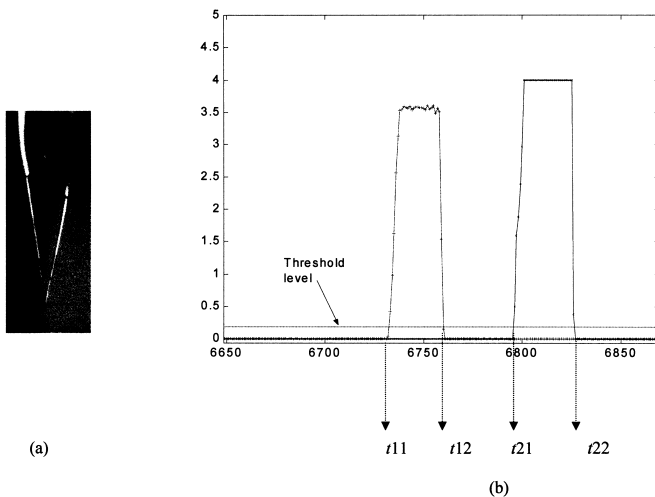


Figure 2. Double optical probe and the time lags from output signals by the two fibres.

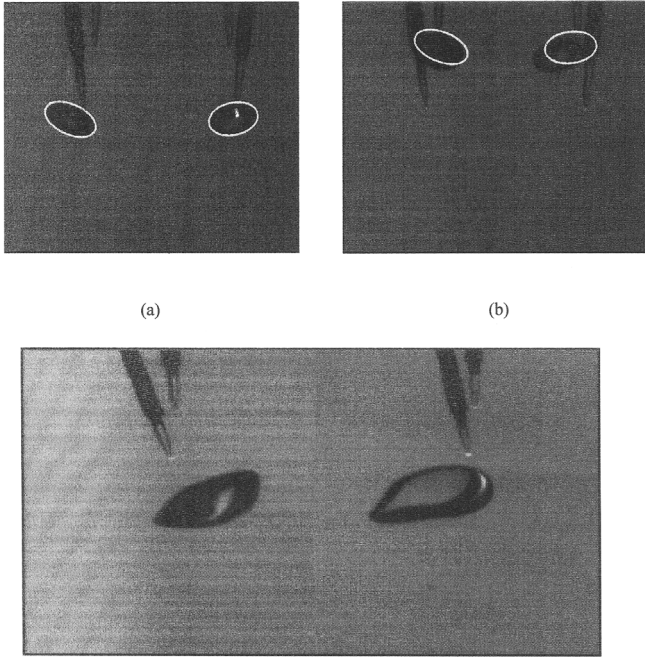


Figure 3. Superimposition of bubble contour and an exact ellipse for bubbles of 2.15mm equivalent diameter.

Image Data Treatment and Analysis

At first, the 0.33mm injector was placed on the bottom of the test tank to produce small bubbles. Rising bubbles are filmed by means of a Kodak Ektapro EM high-speed video system at rate of $1000 \text{ images}\cdot\text{s}^{-1}$. Two cameras perpendicular to tank walls (Figure 1) are used simultaneously to allow a three-dimensional bubble analysis (Figure 1). Filming is performed in such a way that the spatial resolution describes accurately and simultaneously the bubble shape and path. A plane grid of known geometry is filmed to be used for images calibration (conversion of Pixels into mm). A total of 250 bubbles were filmed. After filming, the 0.33mm injector was replaced with the 1mm injector and the same procedure repeated. Only camera setting were adjusted to cater for bubble size.

Images from the two high-speed cameras are digitalized and stored in a computer. A commercial program (Optimas) is used for image processing. The treatment steps include division by background image, filtering, threshold setting and binarisation, erosions and dilations. The bubble contours are finally extracted. The maximum error in bubble contour extraction is about 1 pixel. The bubble centre of mass, the major and minor axis are obtained from bubble contours by aid of homemade software. Two different procedures were used for three-dimensional bubble interface reconstruction.

Reconstruction of Small Bubble Interface

Bubbles from 0.33mm injector have an equivalent diameter of 2.15mm. They are oblate ellipsoids of constant shape. In the bubble motion, the axis of symmetry (minor axis) is parallel to bubble centre velocity (Ellingsen and Risso, 2001). In all cases the measured contour of the bubble was similar to an ellipse with major semi-axis = $1.38 \pm 0.05 \text{ mm}$ and minor semi-axis = $0.72 \pm 0.05 \text{ mm}$.

After initial acceleration, bubbles undergo regular path oscillations. Consequently, the bubble-centre coordinates could be written as:

$$x_G(t) = x_0 + L_x \sin [w_x (t-t_{0x})] \quad (1)$$

$$y_G(t) = y_0 + L_y \sin [w_y (t-t_{0y})] \quad (2)$$

$$z_G(t) = z_0 + L_z \sin [w_z (t-t_{0z})] + \bar{V}_z t \quad (3)$$

where t is the time.

The spatial origins (x_0, y_0, z_0), the time origins (t_{0x}, t_{0y}, t_{0z}), the amplitudes (L_x, L_y, L_z) and the angular frequencies (w_x, w_y, w_z) were determined for each bubble by least square fitting method between measured bubble centre time series and the analytic equations above, until the bubble touches the probe. Details of this procedure are given in Ellingsen and Risso (2001). For a bubble of given size, the parameters of its trajectory are determined : this procedure ensured an accurate determination of the bubble interface. Figure 3a shows superimposition of a filmed bubble and a theoretical ellipse.

Extrapolation of the analytical equations beyond fibres positions is used to analyse the probe impact on the bubble trajectory. During impact, several observations were made : (i) some bubbles were flattened by the probe during piercing, (ii) some bubbles were deviated by the first fibre and never reached the second probe, and (iii) the impact on the first probe provoked sometimes a sudden trajectory change. The last observation is illustrated by Figure 3b.

Thus for small bubbles ($d = 2.15 \text{ mm}$), the shape and the path are well defined and the bubble velocities are obtained by derivatives of the 3 analytic functions above.

Reconstruction of Large Bubble Interface

For larger bubbles however, the procedure described above is no longer valid. In fact according to Perkins and Lunde (1998), bubbles of this size (equivalent diameter 4.5mm) have no constant shape. They exhibit both shape and path oscillations. The shape is rather elongated ellipsoidal and spheroid becoming wobbly and the motion is rocking. This was confirmed by visual observations. Direct bubble shape determination was not possible as only projections on two vertical planes are available (x - z and y - z). An algorithm was developed to obtain the 3 dimensional shape of the bubble at each instant from the two planes (Kiambi, 2003). Figure 4 (a and b) shows the bubble images from the two cameras and the corresponding shape obtained. The validity of this procedure was checked by computing the volume (which should be constant) of the resulting reconstructed bubble shapes. For the same bubble, the volume variation between any two images from the shapes hence obtained was 2% while that between different bubbles was 7%. This variation is reasonable as it incorporates bubble shape changes.

The Virtual Probe

A virtual probe is introduced on the path of each reconstructed bubble shape and the impact times ($t_{11}, t_{12}, t_{21}, t_{22}$) are evaluated numerically from the 3 dimensional analysis of the reconstructed bubble motion past the virtual probe fibres positions. Interfacial bubble velocity (V_{mi}) around the probe is evaluated from the distance (l_{12}) between the 2 probe fibres and the impact times. Bubble residence time on the first fibre, t_R , which leads to gas hold-up and bubble chords lengths, is also

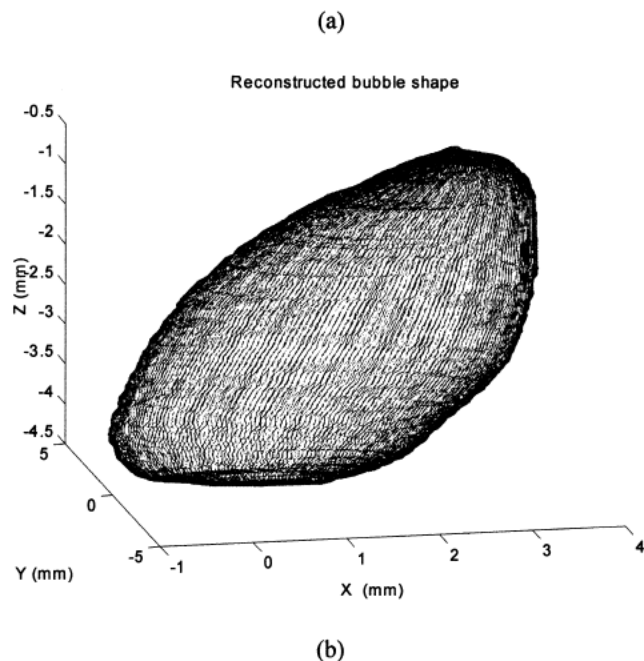


Figure 4. 4.5 mm bubble images and the corresponding reconstructed bubble shape.

evaluated. These parameters from imaging method (virtual probe) are compared with those from the double optical probe (real probe).

Results and Discussion

Bubble Residence Time on the Probe Tips

Since the image analysis method involves the introduction of a virtual probe in the bubble trajectory, the corresponding residence times obtained are free of probe intrusiveness. The theoretical and real bubble residence times of bubbles of 2.15mm equivalent diameter on the real and virtual probe fibres are shown in Figure 5. The corresponding sampled data is presented in Table 1. The acquisition duration of real probe is 19.2 s while that of high speed cameras is only 1.6 s. This explains the differences between samples sizes of real and virtual probes in the table. The difference was partially compensated by use of 9 virtual probes distributed around the central virtual (which is placed at 3.31 mm below the real probe) with a 1.5mm spacing between them. This guaranteed the detection of all bubbles passing in the neighbourhood of the real probe.

The probability density function (PDF) of residence time obtained by the imaging method (virtual fibres 1 and 2) are quite similar since the first probe does not influence the bubble before it reaches the second probe (absence of a physical probe). This similarity indicates that the data converges statistically. The probability density function of bubble residence time on the real fibres are quite different. First of all, the number of bubbles pierced by fibre1 is 30% higher than the second fibre. This clearly depicts the intrusive nature of the optical probe. Secondly, the residence times of the two real fibres are systematically shorter than those of virtual probes. The difference between mean residence time of bubbles on fibre1 of the virtual probe and that on fibre1 of real probe is about $\Delta t_R = 14\%$.

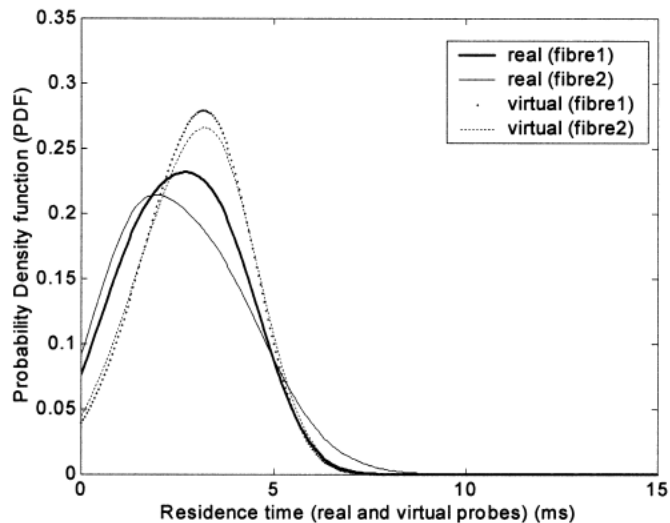


Figure 5. Comparison of residence times of down stream and up stream fibres between real and virtual probes : bubble of 2.15mm.

Real probe	Number of bubbles	Mean residence time
Fibre 1 ($t_{12} - t_{11}$)	1264	2.6
Fibre 2 ($t_{12} - t_{11}$)	865	2.56
Virtual probe		
Fibre 1 ($t_{12} - t_{11}$)	486	2.95
Fibre 2 ($t_{12} - t_{11}$)	519	2.93

Figure 6 shows the PDF of bubble residence times of both real and virtual probes for larger bubbles ($d = 4.5\text{mm}$). Table 2 gives the sample sizes and the average values of the residence times. Here again, the PDF of the first and the second virtual probes are similar. The difference of the mean residence times is only 2.3%. For a larger sample size, 9 virtual probes were also used for bubbles of 4.5mm. The central probe is placed 8.1mm below the real probe and 8 others spaced at 3 mm around the central probe. In Table 2, the second virtual probe pierces more bubble than the first since it is nearer to the real probe: More bubble trajectories cross this point.

Concerning the real probe, the two distributions are rather different. The mean residence time on fibre2 is about 14% smaller than on fibre1. It seems that fibre1 perturbs bubble motion before the piercing by the second fibre. A comparison between the first real probe fibre and first virtual probe fibre shows shorter residence time for the real fibre. The underestimation of about 6% on the mean residence time by the real probe portrays farther the intrusive nature of the real probe.

When a probe is introduced in bubbly flow the void fraction is evaluated as $\alpha = Nbt_{Rm}/T$: where Nb is the number of bubbles

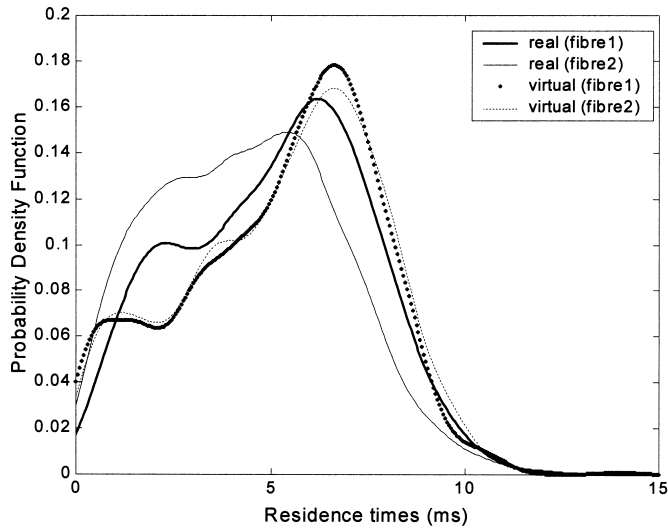


Figure 6. Comparison of residence times of down stream and up stream fibres between real and virtual probes: bubble of 4.5mm.

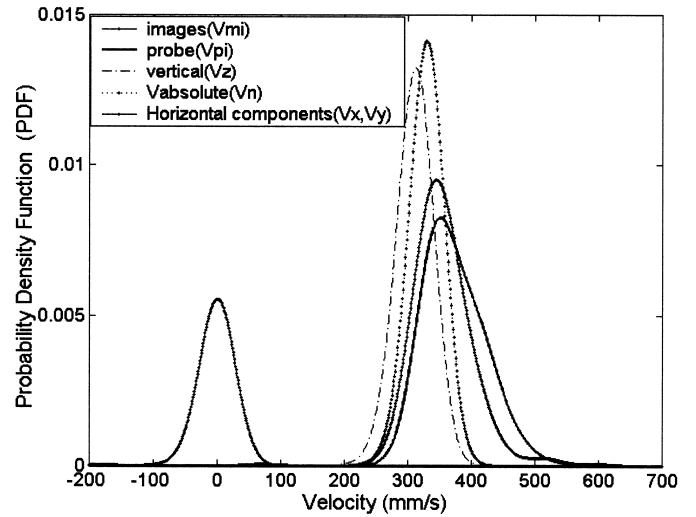


Figure 7. Probability density functions of different bubble velocities (bubbles of 2.15mm).

Table 2. Data of residence time for bubbles of 4.5mm equivalent diameter.

Real probe	Number of bubbles	Mean residence time
Fibre 1 ($t_{12} - t_{11}$)	3367	5.1
Fibre 2 ($t_{22} - t_{21}$)	2545	4.4
Virtual probe		
Fibre 1 ($t_{12} - t_{11}$)	881	5.4
Fibre 2 ($t_{22} - t_{21}$)	1159	5.3

Table 3. Velocity components fir bubbles of 2.15mm equivalent diameter.

Real probe	Number of bubbles	Mean velocity
Interfacial velocity (mm/s)	418	373.30
Virtual probe		
Interfacial velocity (mm/s)	287	355.03
Absolute velocity (mm/s)	187	333.40
Vertical velocity (mm/s)	187	313
Horizontal velocity (mm/s)	187	0

pierced by the first fibre, T being the measuring time and t_{Rm} the average bubble residence time on the first fibre. Then, the relative error on void fraction can be written as :

$$\left| \frac{\Delta \alpha}{\alpha} \right| = \left| \frac{\Delta Nb}{Nb} \right| + \left| \frac{\Delta t_{Rm}}{t_R} \right| \quad (4)$$

The results of this work quantify only the error on mean residence time. The underestimation of 14% for bubbles of 2.15mm and that of 6% on bubbles of 4.5mm shows that the intrusive nature of the double optical probe can be consequential in void fraction determination. Note that the probe is more accurate as the size of bubbles increases.

Bubble Velocity

The PDF of bubble centre velocities for bubbles of $d = 2.15$ mm are represented in Figure 7. Table 3 shows the number of bubbles sampled and the corresponding mean velocities. The advantage of imaging method is that, other velocity components (such as bubble vertical velocity, the magnitude of

the bubble velocity and velocity fluctuations) can be evaluated at each instant along the bubble path. The vertical component of the bubble centre velocity V_z , the horizontal components (V_x , V_y) and the absolute bubble centre velocity V_r are deduced from images.

Interfacial velocities from the probe V_{pi} and from images V_{mi} refer to bubble interface velocity past the real and virtual probes respectively. From Figure 7, real probe gives an interfacial velocity (V_{pi}) higher than the virtual probe (V_{mi}). This difference is probably induced by the bubble path deviations by the first fibre of the real probe. Note that to quantify velocity from an optical probe the bubble must be pierced by the two fibres. It is probable that bubbles ascending vertically are less perturbed by the probe and are more likely to reach the second fibre. This may induce a statistical bias favouring higher vertical velocities. The observations made during bubble piercing also shows that the first fibre provokes sudden bubble directional rotations which could induce vertical bubble accelerations (see Figure 3b). Although

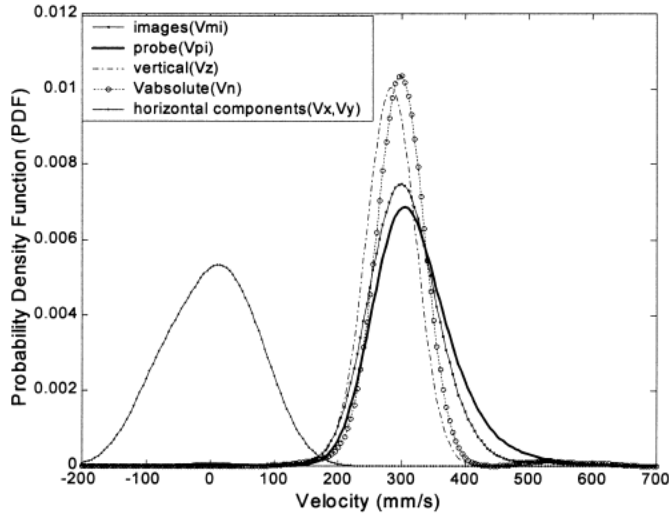


Figure 8. Probability density functions of different bubble velocities (bubbles of 4.5mm).

Real probe		Number of bubbles	Mean velocity
	Interfacial velocity (mm/s)	2041	320.4
Virtual probe	Interfacial velocity (mm/s)	741	305.1
	Absolute velocity (mm/s)	179	300.5
	Vertical velocity (mm/s)	179	287.1
	Horizontal components (mm/s)	358	0

the effect of the probe during impact has been established, its influence on bubble velocity measurements is however limited as shown by the interfacial velocity PDFs on Figure 7. The difference of the average values between virtual and real probe is only 5%.

The interfacial bubble velocity measured by the probe (V_{pi}) includes horizontal, vertical bubble velocities and bubble orientation effects. If the distance between the two fibres (l_{12}) is small compared to the bubble size, the measured interfacial velocity is equal to the actual bubble interface velocity in the vertical direction which is the pertinent velocity for interfacial area transport (Riou, 2002). Normally, the horizontal velocity and bubble orientation effects are on average nil, so the average interfacial velocity is equal to the average bubble centre velocity. This is not the case if the distance l_{12} is the order of the bubble size as in this work. From Figure 7, we also note that the absolute velocity is close to the interfacial velocity of the bubbles.

Figure 8 shows the velocity distributions for the bubbles of 4.5mm and table 4 gives the corresponding bubble number and the average values. As for the small bubbles, the interfacial velocity by real probe is superior than that of the virtual probe. This error of 4.8% is due to the probe interference with the bubble trajectories during impact. Note that the interfacial velocity of large bubbles includes the deformation effects in addition to orientation effects, bubble centre and horizontal velocities.

Conclusions and Perspectives

In this study bubble velocities and bubble residence time on a real and virtual probe tips are compared using image processing method and a double optic probe. Two bubble sizes are considered: bubbles of 2.15 equivalent diameter with regular path oscillations and a constant shape and those of 4.5mm equivalent diameter with irregular trajectories and changing shape. The intrusive nature of the double optical probe has been investigated by means of virtual probes. It has been shown that the optical probes underestimate the void fraction by at least 14% for bubbles of 2.15mm equivalent diameter and at least 6% for bubbles of 4.5mm equivalent diameter.

On the other hand, although the probe perturbs the bubble during piercing, this method can be relied upon for measurements of bubble interfacial velocity. An error of less than 5% was found for the two bubble sizes. The interfacial bubble velocity includes bubble centre velocity component, bubble shape deformations and orientations and horizontal components. If the inter fibre distance is small compared to bubble size, the interfacial velocity can be considered as the velocity for interfacial area transport.

Nevertheless, double optical probe can be relied upon for bubble characteristics measurements especially in highly bubbly unidirectional flows where the bubble translations and rotations effects are minimised by the continuous phase flow. Further studies will be necessary in complex situations such as in high gas hold-up with significant liquid flows.

Nomenclature

i	images subscript
l_{12}	distance between the two probe fibres (mm)
L	amplitude
N_b	number of bubbles
P	probe subscript, (point)
t	time, (s)
t_{11}	arrival time on fibre1, (ms)
t_{12}	departure time on fibre1, (ms)
t_{21}	arrival time on fibre2, (ms)
t_{22}	departure time on fibre2, (ms)
t_R	residence time
T	total measuring period.
V_z	bubble vertical velocity
V_{mi}	interfacial velocity from images
V_n	bubble centre absolute velocity
V_x, V_y	bubble centre horizontal velocity
V_{pi}	interfacial velocity from probes
x, y, z	directions

Greek Symbols

α	gas hold-up
ω	angular velocity

References

- Dias, S.G., F.A. França and E.S. Rosa, "Statistical Method to Calculate Local Interfacial Variables in Two-Phase Bubbly Flows Using Intrusive Crossing Probes", *Int. J. Multiphase Flow*, **26**, 1797-1830 (2000).
- Ellingsen K. and F. Risso, 'On the Rise of an Ellipsoidal Bubble in Water: Oscillatory Paths and Liquid-Induced Fluctuations', *J. Fluid Mech.*, **440**, 235-268 (2001).
- Kamp, A.M., "Écoulements turbulents à bulles dans une conduite en micropesanteur"
Ph.D. Thesis, Institut National Polytechnique de Toulouse, France (1996).
- Kiambi, S.L., "Analyse métrologique de la sonde optique double : interaction sonde-bulle et application en gazosiphon" Ph.D. Thesis, Institut National Polytechnique de Toulouse, France (2003).
- Kiambi, S.L., A.M. Duquenne, A. Bascou and H. Delmas, "Measurements of Local Interfacial Area: Application of Bi-Optical Fibre Technique", *Chem. Eng. Sci.*, **56**, 6447-6453 (2001).
- Kim, S., X.Y. Fu, X. Wang and M. Ishii, "Study on Interfacial Structures in Slug Flows Using Miniaturized Four-Sensor Conductivity Probe", *Nuclear Engineering and Design* **204**, 45-55 (2001).
- Liu, T.J and S.G. Bankoff, "Structure of Air-water Bubbly Flow in a Vertical Pipe: Liquid Mean Velocity and Turbulence Measurements", *Int. J. Heat Mass Transfer* **36**, 1049-1060 (1993).
- Revankar, S.T. and M. Ishii, "Local Interfacial Area Measurement in Bubbly Flow", *Int. J. Heat Mass Transfer* **25**, 913-925 (1992).
- Riou, X., "Contribution à la modélisation de l'aire interfaciale en écoulement gaz-liquide en conduite" Ph.D. Thesis, Institut National Polytechnique de Toulouse, France (2002).
10. Perkins, R.J. and K. Lunde, "Shape Oscillations of Rising Bubbles", *Applied Scientific Research* **58**, 387-408 (1998).